GEOLOGICA CARPATHICA, 2024, 75, 2, 83–97 https://doi.org/10.31577/GeolCarp.2024.07

Distribution of rare earth elements among rock-forming and accessory minerals: A case study of Variscan granites from the Krušné Hory Mts., Czech Republic

KAREL BREITER[1,✉], JANA ĎURIŠOVÁ[1], ZUZANA KORBELOVÁ[1] and MAREK DOSBABA[2]

[1]Institute of Geology, Czech Academy of Sciences, Rozvojová 269, 165 00 Praha 6, Czech Republic
[2]Tescan Orsay Holding a.s., Libušina třída 21, 623 00 Brno, Czech Republic

(Manuscript received April 9, 2024; accepted in revised form June 11, 2024; Associate Editor: Igor Broska)

Abstract: Eight granite samples representing the main petrographic and geochemical types of Variscan granites from the Krušné Hory/Erzgebirge area were studied to decipher the distribution of rare-earth-elements (REE) among all rock-forming, minor, and accessory minerals. The chemical composition (REE contents) of minerals was determined using electron microprobe and laser ablation ICP MS, while the quantitative abundance of individual minerals was determined by automated mineralogy (TIMA technology). Monazite and xenotime + zircon are dominant hosts of both LREE and HREE respectively, especially in strongly peraluminous S-type granites. In less-fractionated Ca-richer facies, allanite is also an important carrier of LREE. In slightly peraluminous A-type granites, monazite + fluorite (including its alteration products) dominates as LREE hosts, while fluorite (including its alteration products), with small contributions of zircon and xenotime, hosts the HREE. The importance of rock-forming silicates for REE distribution is limited; the relatively highest contribution was found in plagioclase (up to approx. 15 % of LREE in S-type granites).

Keywords: granites, rare-earth elements, rock-forming minerals, accessory minerals

Introduction

Group of rare earth elements (REE), due to their specific chemical properties, is of great importance for the interpretation of geological processes (review in Lipin & McKay 1989).

Accessory minerals hosting REE, such as monazite, xenotime, and zircon are generally considered to be the decisive carriers of REE in igneous rocks, and are thus studied frequently, as well as in detail (Broska & Uher 1991; Heinrich et al. 1997; Förster 1998a, b, 2006; Seydoux-Guillaume et al. 2002; Broska et al. 2005; Lindhout 2007; Mogilevsky 2007; Hoshino et al. 2012; Uher et al. 2013; Broska & Kubiš 2018; René 2018). In specific types of granitoids, carriers of significant amounts of REE include allanite, garnet, or fluorite, and such examples are also well-documented (Broska et al. 2000; Ackerman 2005; Schönenberger et al. 2008; Hönig et al. 2014).

Although the contents of REE in rock-forming minerals are several orders of magnitude lower than in the above-mentioned accessory and minor minerals, due to the high representation of rock-forming minerals in the rock, theoretically, they could be an important carrier of REE (Bi et al. 2002; Larsen 2002). This is especially true of dark minerals, pyroxene, and amphibole, which may host a rather important portion of REE; distribution of REE between clinopyroxene and plagioclase, for example, can serve as a geothermometer (Sun & Liang 2017). However, considerably less is known about the REE contents of common light rock-forming minerals like quartz (Götze et al. 2021), feldspar (Cherniak 2003; Ren et al.2003), and micas (Weng et al. 2022).

Attempts to compile a complete REE inventory in granites are indeed rare and are limited to common granitoids (Bea et al. 1994; Bea 1996). Similar data for rare-metal granites are still lacking. Therefore, we decided to analyze the REE contents of all minerals contained in the samples of several representative granites of different geochemical types and grade of fractionation from the Krušné Hory area. The contents of REE were determined using electron microprobe (EPMA) in accessory minerals containing generally more than 0.1 wt.% of individual REEs, as well as by using laser-ablation inductive-coupled mass spectrometry (LA-ICP-MS) in rock-forming silicates. The quantitative representation of individual minerals in the samples was determined using TESCAN technology of automated mineralogy (TIMA). In order to summarize all these data, we attempted to compile a complete REE budget in the studied granites.

Geological characteristics of studied granites and samples

The Variscan granitic rocks in the Krušné Hory/Erzgebirge area (Fig. 1) form a discontinuous belt extending about 160 km along the Czech–German border in a NE–SW direction.

✉ corresponding author: Karel Breiter
breiter@gli.cas.cz

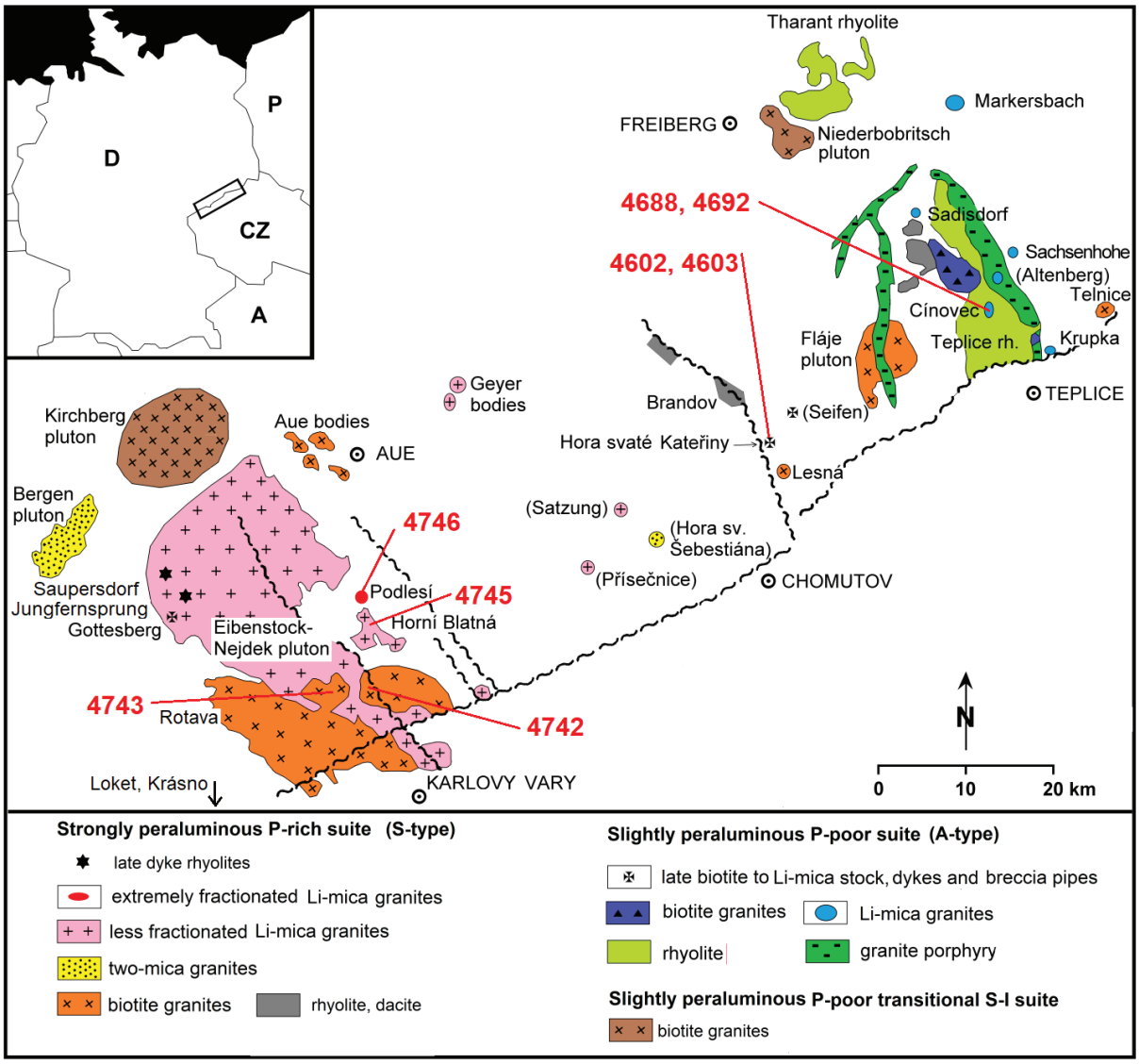

Fig. 1. Distribution of late Variscan granites and volcanic rocks in the Krušné Hory/Erzgebirge with localization of the studied samples. Names of the hidden bodies known only from the boreholes are in parenthesis (modified form Breiter et al. 1999).

The belt comprises about 6000 km^2 and is positioned near the southern border of the Saxothuringian Zone at the NW edge of the Bohemian Massif (Breiter et al. 1999).

The plutonic and volcanic granitoids were emplaced in the late Carboniferous and intruded into folded and metamorphosed lithostratigraphic units, consisting of (from W to E) Ordovician phyllites and quartzites, late Proterozoic–Cambrian mica schists and micaceous gneisses, and Proterozoic paragneisses (Linneman & Rommer 2010).

Relatively bigger, largely eroded plutons (Nejdek–Eibenstock, Bergen, Kirchberg) occur in the southwest, whereas smaller plutons and minor granite stocks (Fláje, Niederbobritz, Schellerhau, Cínovec etc.), complete with voluminous volcanics, are typical for the north-eastern part. Only minor granite stocks (Lesná, Geyer, Hora sv. Kateřiny, Seifen), and several hidden, only in boreholes encountered granite bodies (Satzung, Pobershau, Přísečnice, Hora sv. Šebestiána), were found in the central part of the area.

The characteristic feature of the Variscan magmatism in the Krušné Hory Mts. is the absolute predominance of granites over more basic rocks – the latter comprise less than 1% of the pluton's area on the present erosion surface (biotite diorites to quartz monzonites, "redwizites", according to Kovaříková et al. 2007; lamprophyres according to Seifert 2009).

Variscan granites of the Krušné Hory area have been traditionally divided into two intrusive complexes based on their well-documented relative geological age and spatial relation to tin mineralization: the older intrusive complex (OIC), which consists mainly of barren biotite monzogranites (Loket, Nejdek, Fláje), and the younger tin-bearing intrusive complex (YIC), which ranges from Li-biotite syenogranites with topaz

to albite–zinnwaldite–topaz alkali feldspar leucogranites (Nejdek–Eibenstock, Cínovec, Krupka, Štemprok 1986; Tischendorf 1989). However, recent geochronological data have defined three major episodes of magmatic activity with peaks at 323–318, 315–310 and 300–290 Ma (Table 1; Förster & Rhede 2006; Förster et al. 2008; Tichomirova et al. 2019, 2022).

However, it was not until the 1990s, on the basis of extensive data sets of whole-rock and mineral data, that two geochemically different suites of granites were distinguished, developing in close proximity throughout the entire Variscan magmatic activity. Firstly, Breiter et al. (1991) defined seven chemical types of granites on the Czech side, and then Förster et al. (1999) defined five types of granites on the German side. Both classifications agree in principle on existence of:

- strong, peraluminous suite (A/CNK=1.1 to 1.3), which shows a trend towards enrichment of phosphorus and displays relatively low contents of HFSE and HREE (for simplicity, it is later referred to as S-type granites);
- slightly peraluminous suite (A/CNK=1.0 to 1.1) with a low to very low phosphorus content, increased levels of HFSE and HREE. While the older and less fractionated biotite granites from this suite show transitional S–I chemical composition (Kirchberg pluton, Förster et al. 1999), the younger, more fractionated and closely-related to volcanic activity members show A-type composition.

The majority of the granitic plutons of both geochemical types consist of several intrusive phases with significant fractional crystallization, as well as high to extreme enrichment in lithophile and fluxing elements in the youngest intrusions. Chemical differences between both suites (contents of P, Zr, Y, HREE etc.) are relatively small in the case of less fractionated biotite granites, yet increase strongly during fractionation. At the same time, however, the contents of Li, Rb, Sn, and W increase in both suites, and the most fractionated intrusions of both suites are accompanied by very similar hydrothermal processes and formation of greisen-type Sn–W–Li mineralization.

During the entire magmatic activity, the whole area underwent a fast exhumation; while granites of the oldest intrusive event intruded into a relatively deep crust, the younger magma portions reached close to the Earth's surface, forming subvolcanic bodies, including explosive breccia pipes.

The geochemically primitive peraluminous granites are spread throughout the region and form the relatively large Slavkovský les, Nejdek and Fláje plutons, and smaller bodies at Aue, Lesná, and Telnice. They are mostly medium- to coarse-grained biotite granodiorites to biotite monzogranites or sporadically two-mica monzogranites (only in the Bergen pluton). They are composed of quartz, zoned sericitized plagioclase $An_{15–35}$, poikilitic K-feldspar, biotite, some muscovite, and accessory zircon and apatite. Fractionation in the largest Nejdek pluton produced a small body of fine-grained leucocrate granite at Rotava, but without any enrichment in trace elements.

The younger peraluminous intrusions are widespread mainly in the western half of the area that form the Nejdek–Eibenstock pluton. The main intrusive phase of this pluton consists mostly of medium- to coarse-grained non-porphyritic granites. All facies are characterized by the presence of drop-like quartz and abundant topaz. Based on the degree of fractionation, it is possible to distinguish relatively less-fractionated syenogranites with biotite, oligoclase, and exclusively accessory topaz, as well as strongly fractionated alkali feldspar granites with albite, protolithionite, and topaz over 1%. The youngest intrusive phase forms small stocks of fine- to medium grained albite–zinnwaldite–topaz granites with shows of Sn (+W, Nb, Ta) mineralization, i.e., the cupolas near Krásno (Jarchovský 2006; René 2018) and the stock at Podlesí (Breiter et al. 2005).

The genetic relationship of the swarm of dikes of peraluminous rhyolites/granite porphyry near Jungfernsprung and Saupersdorf in Germany (NW part of the area) to the surrounding 15–20 Ma older Eibenstock pluton is unclear. In any case, these dikes represent the youngest manifestation of Variscan peraluminous magmatism in the Erzgebirge. The pre-caldera Schönfeld rhyolite–dacite volcanism in the eastern Krušné Hory should also be included in the suite of peraluminous magmas; this exhibits a relatively primitive calc-alkaline chemistry and peraluminous character.

The only representative of the older granites with only slightly peraluminous P-poor chemical composition is the Kirchberg

Table 1: Classification of individual magmatic systems in the Krušné Hory / Erzgebirge according to composition and age. The symbols W–C–E indicate the position in the western, central, and eastern sector of the area.

Group of events	Strongly peraluminous suite S-types	Mildly peraluminous suite I- and A- types
3	291±11 Mahnbruck (W) 295±20 Jungfernsprung (W)	295±15 Gottesberg (W) 301±5 Seifen (C) ?? Hora svaté Kateřiny (C)
2	312–310 Podlesí (W) 315–312 Horní Blatná (W) 315–314 Eibenstock (W) ?? Geyer–Ehrenfriedersdorf (C)	<312 post-caldera granites (E): Schellerhau, Cínovec, Krupka, Altenberg etc. 312 caldera dikes (E) 314–313 Teplice rhyolite (E)
1	320–318 Bergen (W) 322 Schonfeld volcanic (E) 323–322 Aue (W) ?? Nejdek (W), Fláje (E), Telnice (E), Lesná (C)	320–318 Niederbobritsch (E), 320–318 Kirchberg (W) 322 Schonfeld volcanic (E)

pluton in Germany. It consists chiefly of medium-grained porphyritic biotite granite. It can be classified as S–I transitional geochemical type (Förster et al. 1999).

The extrusive-subvolcanic complex of Altenberg–Teplice Caldera (ATC, Breiter 1997; Tomek et al. 2019) in the eastern part of the area geologically divided the older group of peraluminous biotite granites (Fláje, Niederbobritsch), and the younger group of A-type tin-bearing intrusion emplaced after the caldera collapse. Intrusions of biotite granites with topaz (plutons of Schellerhau and Preiselberg) were followed by a number of small subvolcanic stocks of albite–zinnwaldite–topaz granites with tin mineralization in Altenberg, Cínovec/Zinnwald, Sadisdorf, and Krupka. The characteristic features of these rocks are increased contents of zircon, monazite, thorite, xenotime, uraninite, pyrochlore, and other minerals of REE and Nb–Ta (Johan & Johan 1994, 2005; Förster 2006; Breiter et al. 2017).

Small granite stocks of a similar A-type chemical composition were recently found in the central part of the Krušné Hory Mts. near Seifen (Förster & Rhede 2006) and Hora svaté Kateřiny (Breiter 2008). Dikes of P-poor rhyolites and microgranites near Gottesberg, which are well-known from the adjacent tin mine where they intrude the S-type granites of Eibenstock pluton, were also identified as A-type rock (Wasternack et al. 1995; Förster et al. 2007). All of these small intrusions were formed during the last magmatic episode at ca. 300 Ma.

Eight typical samples representing the main granite types of both geochemical suites were selected for detailed study of contents and distribution of REE. Their basic description is included in Table 2.

Methods

Whole-rock chemical composition

The whole-rock (WR) major element oxide analyses (wet technique) were performed at the Czech Geological Survey, Praha. Replicate analyses of international reference material (JG-3; Geological Survey of Japan) yielded an average error (1 sigma) of ±1 % with respect to the recommended values. Trace elements, including REE, were determined by ICP mass spectrometry following lithium metaborate/tetraborate fusion or nitric acid digestion in the laboratory of Bureau Veritas Mineral laboratories, Vancouver, Canada (for details see http://acmelab.com/)

Automated mineralogy (TIMA)

A TESCAN Integrated Mineral Analyzer (TIMA) based on a TESCAN MIRA FEG-SEM platform in the demonstration facility of TESCAN ORSAY HOLDING in Brno, the Czech Republic was used for automated mineralogical, modal, and textural analyses. This included collection of backscattered electron (BSE) and energy dispersive (EDS) data on a regular grid of 10 μm point spacing. 1000 counts per pixel were acquired using the high-resolution mode. Acceleration voltage of 25 kV and a beam current of 10 nA were used during the data acquisition. The individual points were grouped based on a similarity search algorithm, and areas of coherent BSE and EDS data were merged to produce segments (i.e., mineral grains). Individual spectra from points within each segment were summed. Data from each segment were then compared against a classification scheme to identify the mineral and assign its chemistry and density. The results were plotted as a map showing the distribution of minerals within each individual sample (Hrstka et al. 2018).

Electron probe micro analyze (EPMA)

The composition of allanite, apatite, fluorite, monazite, xenotime and zircon was determined using a Jeol JXA-8230 electron microprobe operated in wavelength-dispersive mode and housed in the Institute of Geology of the Czech Academy of Sciences, Praha. All details of measurements parameters are referenced in the Supplementary Table S1. The counting times on each peak were optimized for individual elements according to their expected concentrations. X-ray lines and background offsets were selected to minimize interference. The PRZ

Table 2: Basic characterization of samples.

Geochemical affiliation	Geological affiliation	Locality	No.	Rock classification
strongly peraluminous S-type	OIC of the Nejdek pluton	Dračí skála outcrop	4742	biotite granite
		Tisovský vrch outcrop	4743	biotite granite
	YIC of the Nejdek pluton	Horní Blatná body, Černá voda valley	4745	topaz-Li-mica-albite granite
		Podlesí stock, quarry	4746	topaz-Li-mica-albite granite
mildly peraluminous A-type	Hora svaté Kateřiny stock	Hora svaté Kateřiny	4603	albite-Li-mica granite, hydrothermally altered
			4602	albite-Li-mica granite, fresh
	Cínovec pluton	borehole CS-1, depth of 988m	4692	biotite granite
		borehole CS-1, depth of 559m	4688	zinnwaldite granite

correction procedure (XPP method metal/oxide, Ritchie 2009) was applied. Empirically determined correction factors were applied to the overlapping X-ray lines.

Empirical formulae were calculated on the basis of appropriate amounts of atoms of oxygen in a formula unit (apfu). Detection limits are included in tables of analytical results.

Laser ablation inductively coupled plasma mass spectrometry (LA-ICP-MS)

Trace element concentrations in feldspars and micas were analyzed using an Element2 ICP-MS (Thermo Fisher Scientific) coupled to an Analyte Excite 193 nm excimer laser ablation system (Teledyne/Cetac) at the Institute of Geology of the Czech Academy of Sciences, Praha.

Samples were ablated in spots of 100 µm diameter. The laser was fired at the repetition rate of 20 Hz and a fluence of 7 J/cm^2. The isotopes ^{7}Li, ^{29}Si, ^{139}La, ^{140}Ce, ^{141}Pr, ^{146}Nd, ^{147}Sm, ^{153}Eu, ^{157}Gd, ^{159}Tb, ^{163}Dy, ^{165}Ho, ^{166}Er, ^{169}Tm, ^{172}Yb and ^{175}Lu were measured at the low mass resolution mode and ^{23}Na, ^{28}Si, ^{39}K were measured at the medium mass resolution mode. Each analysis included acquisition of 15 s gas blank and 25 s laser ablation signal. The calibration standard NIST SRM 612 was analyzed before and after each set of 10 unknowns. Si and its concentrations obtained by electron microprobe were used as the internal standard. The time-resolved signal data were processed using the Glitter software (Achterbergh et al. 2001).

Results

Chemical composition of granites

Results from the whole-rock chemical analyzes of the studied granites are shown in Supplementary Table S2.

From a geochemical point of view, older intrusions of both geochemical types correspond roughly to high-K calc-alkaline granites (Štemprok et al. 1986; Tischendorf 1989; Breiter 2012). Their fractionation is reflected in the increase of Si content and in the depletion of Ti, Mg, Fe, Ca, Sr, Ba, Zr and REE. The contents of lithofile elements (Li, Rb, F) increase only slightly. Even within the groups of younger intrusions, the contents of major elements and their evolutionary trends in both geochemical granite suites are similar – a gradual increase in Al, Na and F, and decrease in Si. The contents of Ti, Mg, Fe and Ca are low from the very beginning of fractionation.

There is a significant difference in phosphorus levels. In strongly peraluminous granites, the phosphorus content increases systematically (from 0.2 to 1.5 wt.% P_2O_5) and these granites can thus be simply described as "phosphorous" (Taylor & Fallick 1997). On the other hand, in slightly peraluminous granites, phosphorus is always very low — below 0.05 wt.% P_2O_5. The phosphorus content naturally has an impact on the crystallization of accessory minerals and consequently on the behavior of many trace elements during fractionation. While an increase in the content of lithophile elements (Li, Rb, Cs, Ga, F) and also of Sn, W, Nb and Ta are common for both geochemical types of granites, there is a substantial difference in the behavior of Zr, Th, Y and REE. Their contents decrease in peraluminous (and thus P-rich) S-granites, but increase in slightly peraluminous phosphorus-free A-granites. The degree of fractionation in the granites from Krušné Hory Mts. is very high, if commonly used indicators of fractionation are considered – Rb/Sr evolved from 1 to over 100, Zr/Hf from 40 to 10, U/Th from 0.1 to 10 (Supplementary Table S2).

The behavior of REEs in both granite suites is different. In the strongly peraluminous suite, the sum of REEs reaches about 200 ppm in the early biotite granites of the Nejdek pluton, and systematically decreases to 10–15 ppm in the most fractionated Li-rich granite facies from Podlesí. The predominance of LREEs over HREEs decreased during fractionation from Ce/Yb(CN)=16–20 to 3–4 and the distribution curve thus flattened. A negative Eu-anomaly as well as its deepening during fractionation is typical (Fig. 2).

Rocks of the slightly peraluminous suite contain ca. 140–260 ppm REEs through the whole magmatic evolution; this content decreased only during late metasomatic processes.

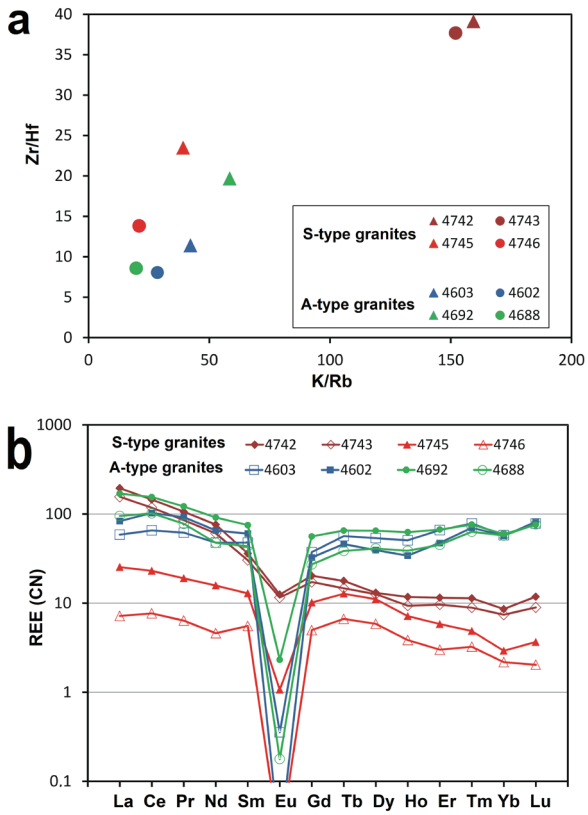

Fig. 2. Whole-rock chemical composition of granites: **a** — evolution grade of studied rocks expressed as K/Rb vs. Zr/Hf diagram; **b** — chondrite-normalized REE patterns.

The distribution curve is generally flat during the whole suite evolution (Ce/Yb(CN)=1–2), and a negative Eu-anomaly is strong.

Modal composition of granites

The mineral composition of the studied granites was determined using the TIMA method; the results are summarized in Supplementary Table S3 and shown in Figs. 3 and 4. Generally, the most common mineral is quartz (24.0–39.7 wt.%) followed by plagioclase (oligoclase to albite, 22.8–35.1 wt.%), K-feldspar (mostly perthitic orthoclase, 19.7–29.7 wt.%), and micas evolving from annite to zinnwaldite (3.0–7.8 wt.%). Minor constituents are apatite (0.15–0.30 wt.%) and topaz (0–4 wt.%) in strongly peraluminous granites, and fluorite in mildly peraluminous ones (0.06–0.53 wt.%). However, it cannot be forgotten that in the case of coarse-grained rocks, the size of thin sections is rather small to give statistically significant modal composition.

Among magmatic accessory minerals, the relatively most common one is zircon (up to 0.05 wt.%). Among REE-bearing phosphates, monazite distinctly prevails over xenotime. Allanite was found only in less evolved peraluminous granites of the OIC Nejdek pluton. The mildly peraluminous granites, which are relatively richer in REEs, contains tiny aggregates of secondary carbonates and fluorocarbonates of REE as well (bastnäsite and synchysite type) with a highly variable chemical composition, usually too small to be analyzed.

Plagioclase

Acid plagioclase is, after quartz, the second most represented mineral in all of the samples (22.8–35.1 wt.%); its abundance generally increases with increasing fractionation in both granitic suites. The composition of plagioclase corresponds to oligoclase in biotite granite of the Nejdek OIC, while all of the other granites contain albite. The contents of An-component shrinks to <1 % in the most fractionated facies. Oligoclase from the biotite OIC granites forms common phenocryst (5–10 mm across), while albite in other granite types appears namely as a late mineral in the matrix.

The highest total content of REE, between 30–50 ppm, was found in oligoclase from biotite granite of the Nejdek OIC (Supplementary Table S4). Albites from Cínovec and Hora sv. Kateřiny contain an average of 10 ppm (2–20 ppm in individual spots) and albite from the Li-mica YIC Nejdek granites usually less than 5 ppm of the sum of the REEs. The chondrite normalized REE distribution curves show strong predominance of LREE over HREE (La/Lu up to 100, Fig. 5a) with positive Eu anomaly in the biotite OIC granites and negative Eu-anomaly in all of the other granite types.

K-feldspar

K-feldspar (usually close to orthoclase) is somewhat less present than plagioclase in the range of 19–30 wt.% without any general trend during fractionation. It is mostly represented as perthite phenocrysts and generally crystallized before plagioclase/albite. The content of unmixed Ab-component decreases from 10–20 wt.% in biotite OIC granites to <5 wt.% in Hora sv. Kateřiny and Podlesí.

The content of REE in K-feldspar is distinctly lower than in plagioclase: the relatively highest totals were found in Cínovec and in Nejdek OIC (4 ppm); the lowest (<1 ppm) in Li-mica granites of the Nejdek–Eibenstock pluton (Supplementary Table S5). Even in this case, the LREE prevail over HREE (La/Lu_{CN}=10–100, Fig. 5b).

Analytical remark: Ablation spots reaching Ab-admixtures were not considered. Due to the low contents of Eu and Gd and simultaneous presence of Ba, it was not possible to analyze these elements in all of the samples properly.

Trioctahedral micas

The highly dominating micas in the studied granites are Fe-micas of annite–siderophyllite type with contents of Li increasing during fractionation reaching zinnwaldite at Cínovec (#4688) and Podlesí (#4746). The modal content of mica varied between 3–7.8 wt.%. In general, mica is a late mineral crystallizing between larger grains of quartz and feldspars.

The content of REE in the analyzed mica is very low (Supplementary Table S6) — about 4 ppm of the sum of REE was found at Hora sv. Kateřiny (#4603), 1–4 ppm in biotite granites of Nejdek OIC, and values <1 ppm prevails in other samples. The contents of Eu and HREE are often below detection limits. If most of the REE could be properly analyzed, the chondrite-normalized curves would be rather flat with a deep Eu anomaly (Fig. 5c).

Allanite [$Ca(REE,Ca)Al_2(Fe^{++},Fe^{+++})(SiO_4)(Si_2O_7)O(OH)$]

In generally Ca-poor granites of the Krušné Hory area, allanite is a rather scarce mineral. It was found only in biotite granites of the Nejdek OIC (0.012 wt.% in sample 4743) as small columnar grains, max 120×40 μm, mostly embedded in mica (Fig. 6a). The most represented REE are La and Ce (about 6 wt.% La_2O_3 and 13 wt.% Ce_2O_3, Supplementary Table S7), while the contents of HREE are usually below detection limits.

Fluorite [CaF_2]

Magmatic fluorite is a typical minor mineral of granites of the slightly peraluminous A-type suite (0.1–0.5 wt.%). It is the main carrier of F and Ca in these granites, and also an important host of Y and REE. It forms euhedral to anhedral grains up to 1 mm across (Fig. 6i). If kept in its primary state, it contains up to 7.6 wt.% of sum of REEs (Supplementary Table S8); the chondrite-normalized distribution curve is, in such case, flat (Fig. 5f). However, fluorite is commonly altered during the hydrothermal stage, and liberated REEs form, after

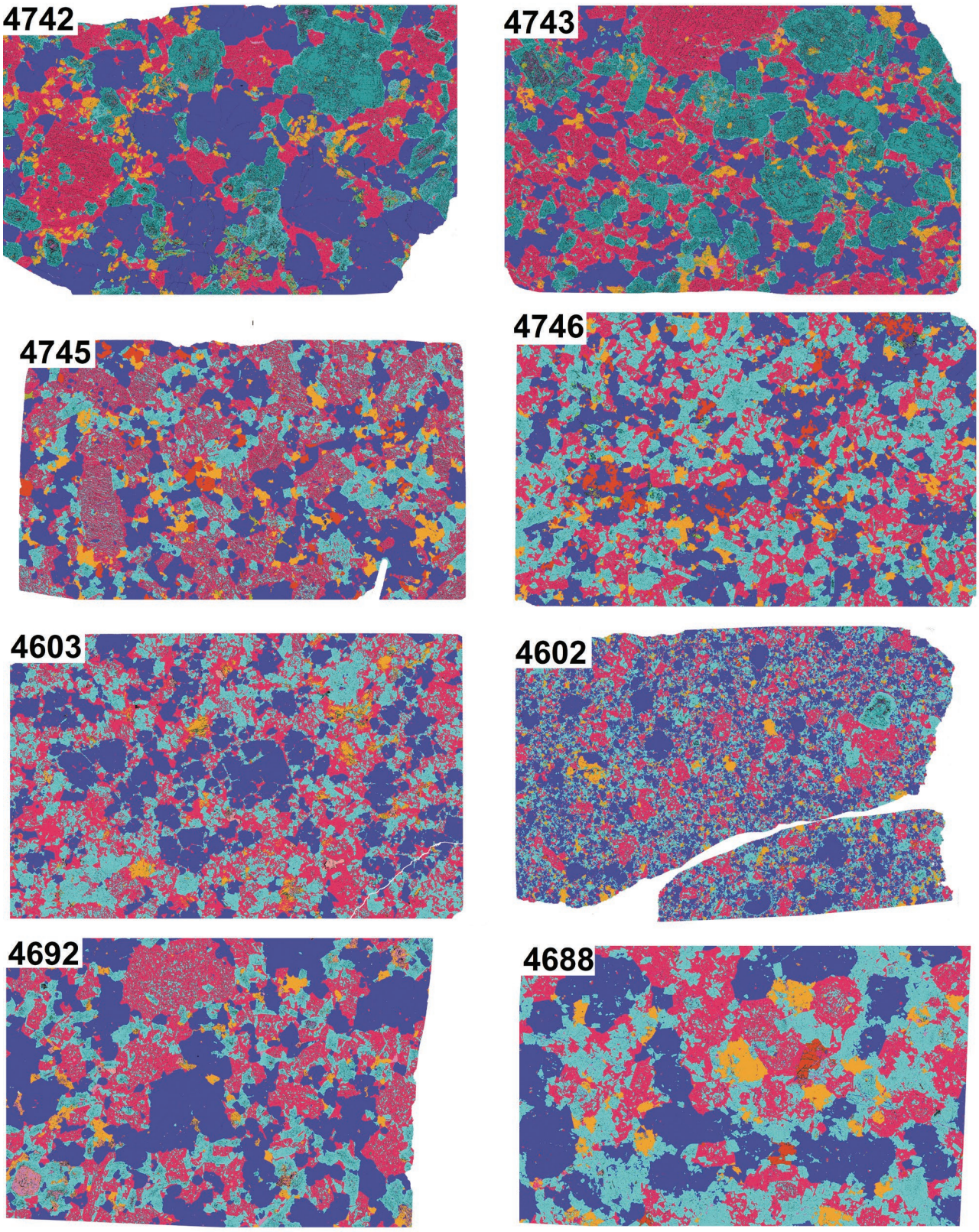

Fig. 3. TIMA mineral maps of the studied samples. Explanation of colors: dark blue – quartz, light blue – plagioclase, red – K-feldspar, orange – micas.

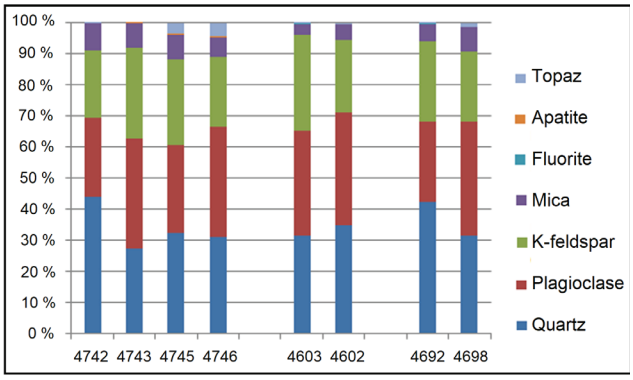

Fig. 4. Modal composition of granites according to TIMA. Only minerals with content >1 wt.% are shown.

only minimal transport, an assemblage of REE carbonates and fluorocarbonates with bastnäsite as the most common member. While the LREEs are liberated more easily, the altered fluorite has a typical left-bowed REE-distribution curve (Fig. 5f).

Apatite [$Ca_5(PO_4)_3F$]

Apatite (in all cases fully F-saturated fluoroapatite) is a typical minor mineral in P-rich strongly peraluminous granites of the Nejdek–Eibenstock pluton (0.15–0.30 wt.%, Supplementary Table S3). It usually forms rounded grains embedded in, or associated with mica (Fig. 6b). A common constituent of igneous apatite is Mn, whose content generally increases during fractionation – in the case of Nejdek pluton from ca. 1 to 2 wt.% MnO. Studied apatites are REE-poor – the sum of LREE (La, Ce, Nd, Sm) does not exceed 0.25 wt.% of REE_2O_3, and during fractionation even decreases (Supplementary Table S9). The contents of other REEs are below the EPMA detection limit.

Monazite-(Ce) [$CePO_4$]

Monazite is the most common host of LREE in granites. It was found in all of the studied samples in an amount roughly proportional to the total REE content in the rock (0.003–0.018 wt.%, Supplementary Table S3). Monazite usually forms small (<50 μm), rounded, or irregularly shaped grains, often associated with apatite, xenotime, or zircon and embedded in biotite or Li-mica (Fig. 6d, f, g).

The monazite structure strongly preferred LREE over HREE, forming a typical right-bowed REE-distribution curve (Fig. 5d). The contents of individual LREE varied between 6.7–14.9 wt.% La_2O_3, 20.0–34.3 wt.% Ce_2O_3, 2.0–4.3 wt.% Pr_2O_3, and 9.2–13.7 wt.% Sm_2O_3 (Supplementary Table S10). The content of Th (i.e., cheralite component) varied between 3.67 wt.% ThO_2 at Hora sv. Kateřiny (#4603) up to 18.04 wt.% ThO_2 (#4745) in Li-mica granite of the Nejdek YIC. Monazite from the Nejdek YIC is also enriched in U (2.2–2.5 wt.% UO_2), while other granites contain monazite with less than 0.5 wt.% UO_2. The contents of Y and HREE are relatively low, but substantially higher in fractionated peraluminous granites from Nejdek pluton than in fractionated A-type granites from Hora sv. Kateřiny (Fig. 7a).

Xenotime-(Y) [YPO_4]

Xenotime is an important host of HREE in granites. It was found in the majority of the studied samples in an amount of a max. 0.0054 wt.% in biotite granite from Cínovec (Supplementary Table S3). Distribution of xenotime in rocks is highly uneven, and its modal content, measured by TIMA, does not correlate with the bulk-rock contents of HREE (compare Supplementary Tables S2 and S3). Xenotime usually forms irregular, but internally zoned grains, individual or associated with zircon, and rarely with monazite. In both cases, xenotime is younger (Fig. 6d, g, h). At Hora sv. Kateřiny, xenotime was extensively replaced by chernovite (Fig. 6d). The contents of Y varied between 28.1 and 43.9 wt.% Y_2O_3 in a negative correlation with HREE (2.0–6.3 wt.% Dy_2O_3, 2.5–4.9 wt.% Er_2O_3, 1.8–9.5 wt.% Yb_2O_3, Fig. 7b, c, Supplementary Table S11). Higher contents of HREE were found in mildly peraluminous A-type granites. The right growing distribution curve for xenotime is typical (Fig. 5e).

Chernovite [$YAsO_4$]

Chernovite is a relatively scarce mineral, recently found in some hydrothermally-altered fractionated A-type granites (Ondrejka et al. 2007; Breiter et al. 2009). It occurs in some domains of Hora sv. Kateřiny granite altered in the presence of As-enriched fluid (Fig. 6d, e). Chernovite is isostructural with xenotime, and behavior of REE in chernovite is thus analogous to those in xenotime (Fig. 5e, Supplementary Table S11).

Zircon [$ZrSiO_4$]

Zircon is another host of HREE and a common accessory in all granite types (0.01–0.05 wt.%, Supplementary Table S3). Zircon forms predominantly euhedral-subhedral crystals, often with internal zoning and is commonly associated with xenotime, chenovite, or monazite (Fig. 6c, e, f, g, h, i). It often forms inclusions in mica, but may also be embedded in fluorite or in the matrix. Zircon, which is isostructural with xenotime, prefers HREE to LREE. The studied samples contain up to 7.1 wt.% Y_2O_3, 3.1 wt.% Yb_2O_3, 1.5 wt.% Er_2O_3, and 1.2 wt.% Dy_2O_3, while the contents of LREE are usually below detection limits (Supplementary Table S12). The contents of HREE in zircon correlate well with their bulk-rock contents, being much higher in zircon from the A-type granites from Hora sv. Kateřiny and Cínovec as compared to the zircon from the peraluminous Nejdek pluton (Fig. 7d).

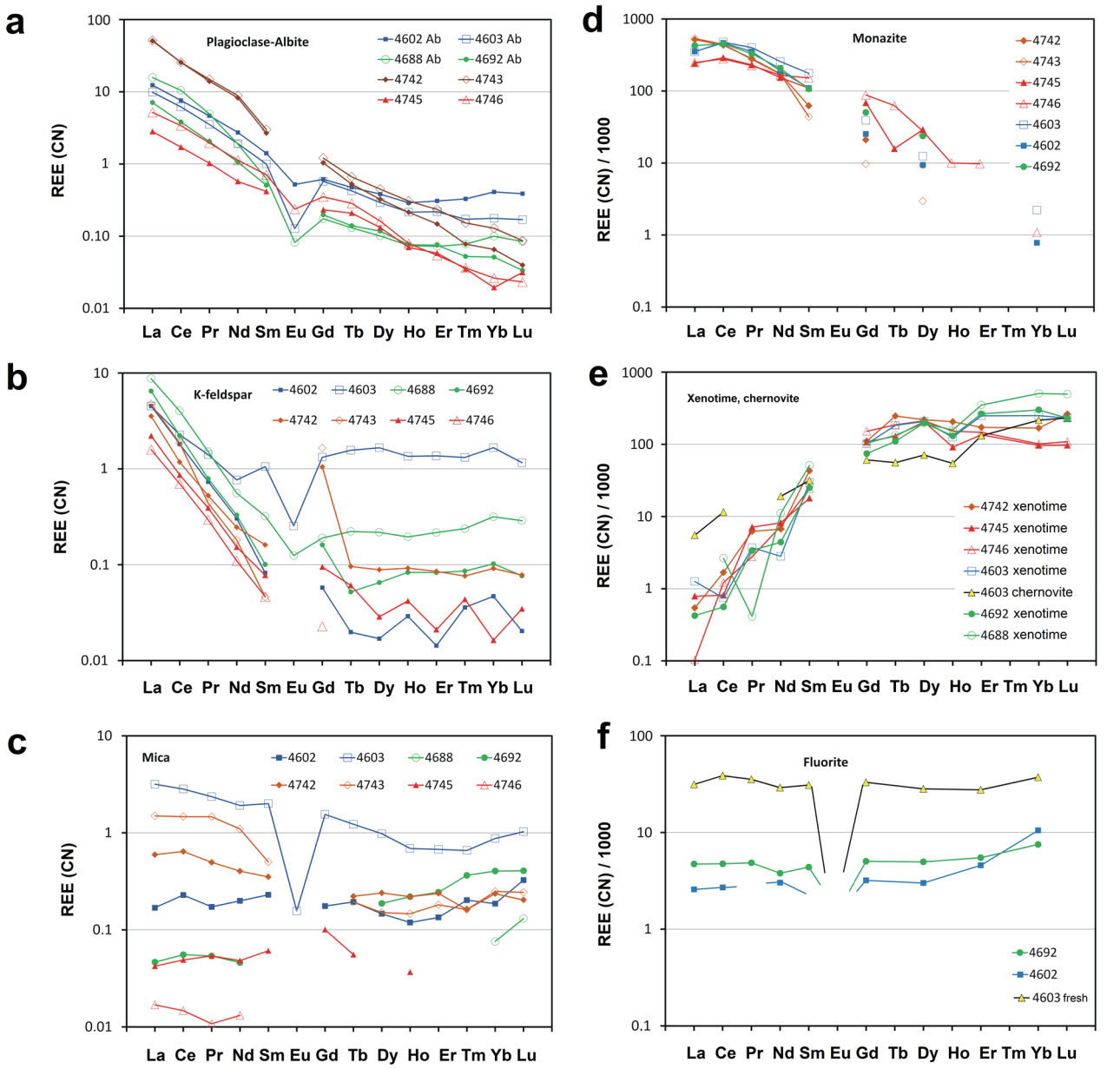

Fig. 5. Chondrite-normalized REE patterns of minerals: **a** — plagioclase; **b** — K-feldspar; **c** — micas; **d** — monazite; **e** — xenotime and chernovite; **f** — fluorite. REE in fluorite sample #4692 acc. to unpublished data by S. Hreus.

Other REE-phases

To a varying degree, the hydrothermally-altered samples from Cínovec and Hora sv. Kateřiny (in particular #4688 and 4603) contain fine aggregates of REE carbonates/fluorocarbonates/oxyfluorides of a highly variable composition that are usually associated with altered fluorite. According to the qualitative analysis, the phases close to synchysite ($CaCe(CO_3)_2F$) or bastnäsite ($Ce(CO_3)F$) prevail, however, small dimensions of the grains did not allow a reliable quantitative analysis.

Discussion

REE in fluorite

The contents of REE in hydrothermal fluorite of different affiliation (vugs or veins enclosed in carbonatites, pegmatites, alkaline rocks, Mississippi-Valley-Type deposits) are well-constrained. The published contents are generally small, varying in the order of tenths or units of ppm of individual REEs (Möller et al. 1976; Schwinn &Markl 2005; Trinkler et al. 2005; Makin et al. 2014).

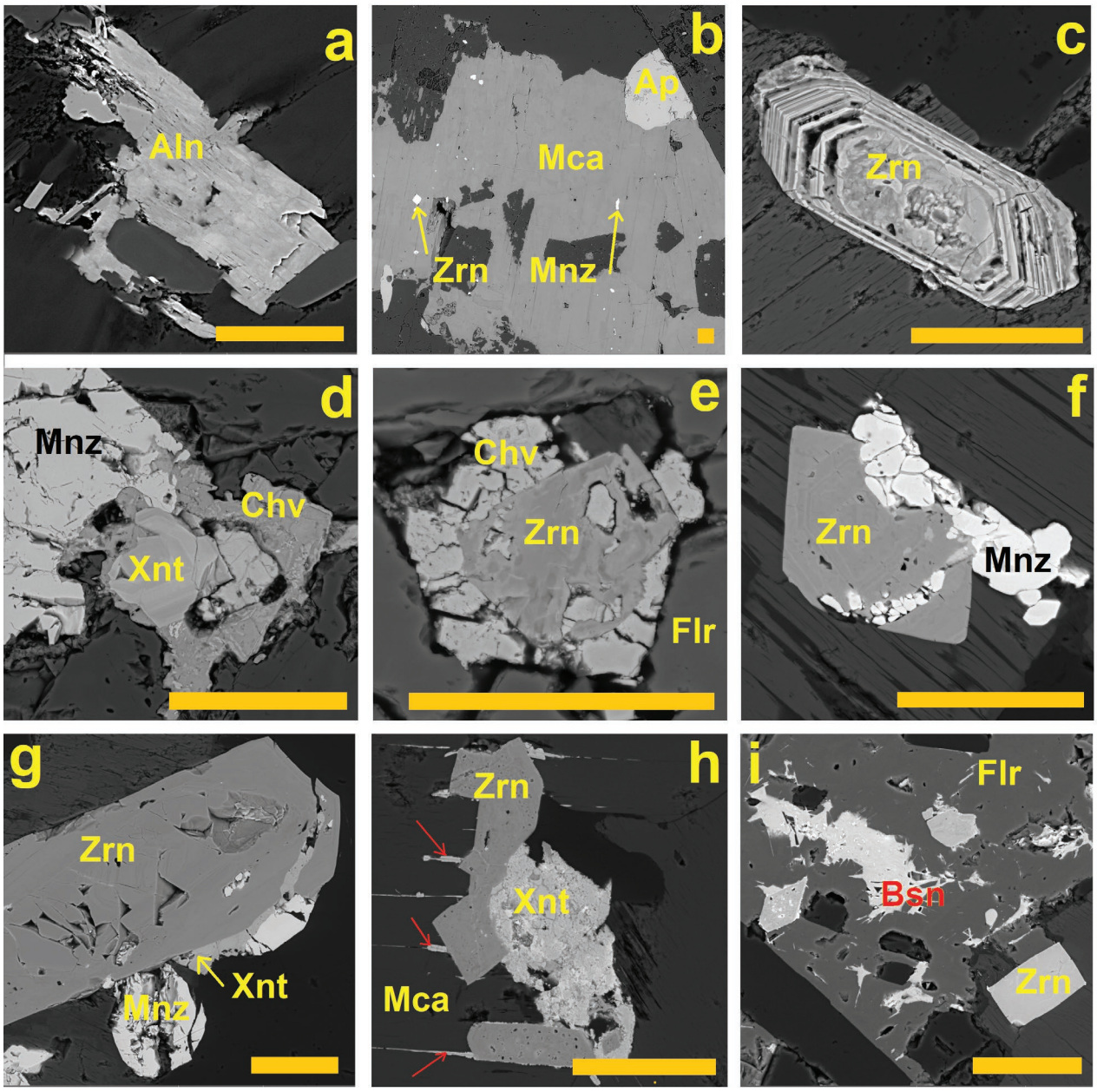

Fig. 6. Back-scattered electron images (BSE) of accessory minerals hosting REE: **a** — allanite hosted in biotite (#4743), biotite granite of the Nejdek pluton; **b** — apatite, zircon and monazite as inclusions in mica, common assemblage in all peraluminous granites (#4745), Li-biotite–topaz granite of the Nejdek pluton; **c** — zoned zircon crystall hosted in biotite (#4742), biotite granite of the Nejdek pluton; **d** — association of monazite with xenotime hosted in feldspar, partly replaced with chernovite (#4603), Li-biotite granite of the Hora sv. Kateřiny stock; **e** — zircon rimmed with chernovite hosted in fluorite (#4603), Li-biotite granite of the Hora sv. Kateřiny stock; **f** — zircon associated with monazite, hosted in biotite (#4692), biotite granite of the Cínovec pluton; **g** — zircon associated with monazite, late xenotime fills rupture of the zircon crystal (#4692), biotite granite of the Cínovec pluton; **h** — zircon associated with altered xenotime, late xenotime penetrates mica along cleavage (highlighted with red arrows, #4688), zinnwaldite granite of the Cínovec pluton; **i** — altered fluorite associated with zircons, REE liberated from fluorite immediately formed bastnasite-like mineral phases (#4688), zinnwaldite granite of the Cínovec pluton. Scale bars 50 μm in all cases.

Crystallization of primary magmatic fluorite is restricted to highly-fractionated and strong, F-enriched silicic melts (Li et al. 2020) which often produce so-called rare-metal granites. Fluorite is easily saturated in metaluminious melt with (Na+K)→1 (Scaillet & Macdonald 2004), although data on its REE capacity from nature are scarce. Schönenberger et al. (2008) referred 423 ppm Y, 120 ppm La, 243 ppm Ce, and 9 ppm Yb among others from the paralkaline Ilímaussag compex, Greenland, and Badanina et al. (2006) found in fluorite from another F-rich granite system at Orlovka, Siberia, highly

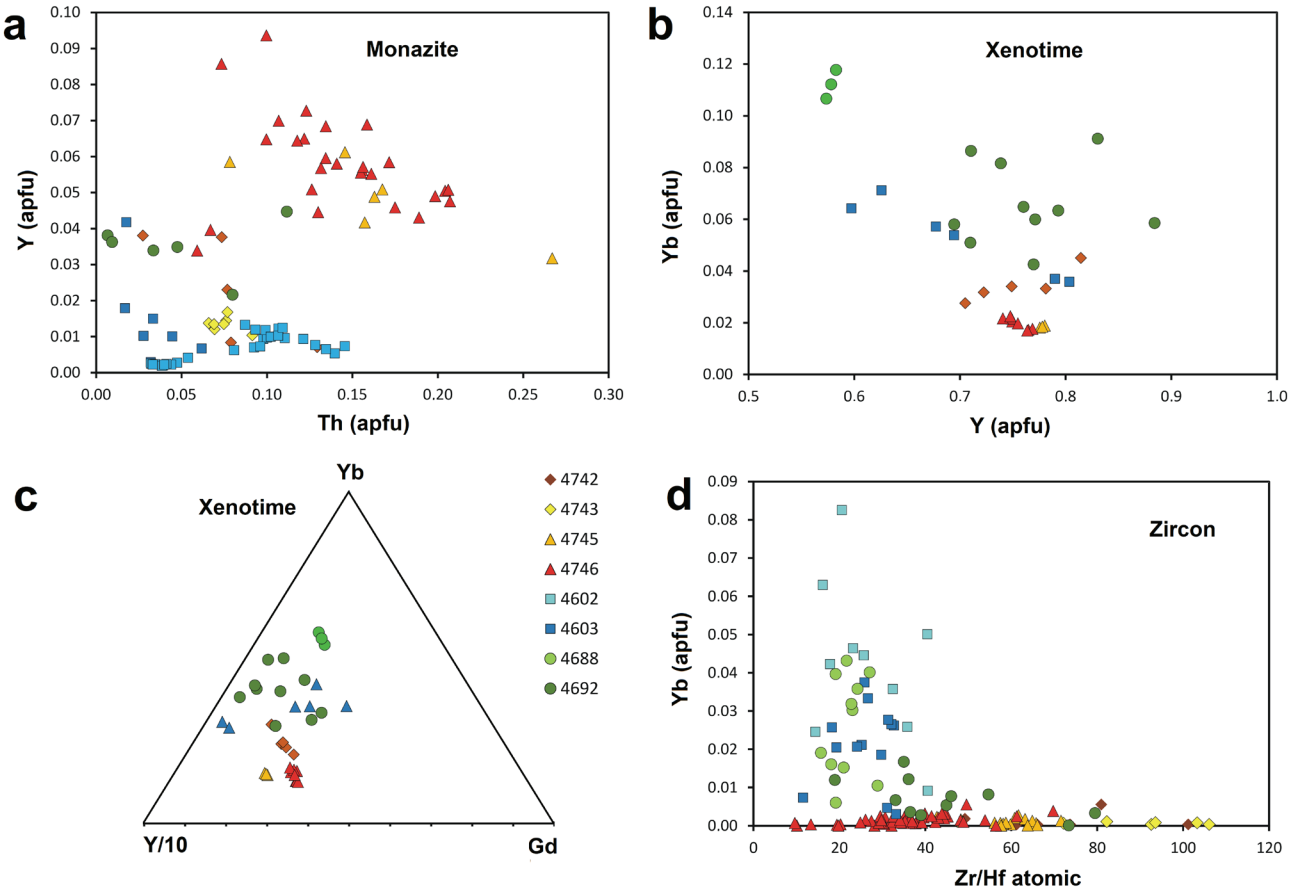

Fig. 7. Chemical characteristic of accessory minerals: **a** — Th vs. Y contents in monazite; **b** — Y vs. Yb contents in xenotime; **c** — relation between contents of Y, Gd and Yb in xenotime; **d** — relation between Zr/Hf value and Yb content in zircon.

variable contents in the range 0.6–264 ppm La, 1–894 ppm Ce, 0.7–385 ppm Gd, 1–446 ppm Yb among others. All referred values are by one to two orders of magnitude less than the values found at Hora svaté Kateřiny and Cínovec.

Experiments performed by Veksler et al. (2005) indicate 100–200 times REE-enrichment in coexisting fluoride to hydrous silicate melt; crystallization of extreme Y,REE-rich fluorite in A-type granites may indicate at least local unmixing of fluoride melt during fast cooling of F-rich melt reaching strong PT-gradient in subvolcanic conditions at Cínovec and Hora svaté Kateřiny.

REE in feldspars

Bea et al. (1994) found ca. 7–9 ppm La, 13–15 ppm Ce, and 1.7–2.9 ppm Eu in plagioclase, and ca. 1.7–2.5 ppm La, 3.0–4.3 ppm Ce, and 1.1–1.8 ppm Eu in associated K-feldspar from common granites. The REE-contents found in Krušné Hory are similar or somewhat smaller. The important difference is negative Eu-anomaly in the most of feldspar from Krušné Hory granites indicating evolved parental melt of studied granites, already strongly depleted in Eu during previous fractionation.

REE in micas

Bea et all. (1994) found in studied samples of granitic biotite less than 1 ppm of individual REEs (LREE>>HREE). In syenite–carbonatite complex at Maoniuping, China, magmatic Fe-mica contains 0.X–5 ppm of individual REEs, however, late hydrothermal mica contains up to 77 ppm of total REE with strongly prevailing LREE (Weng et al. 2022). In respect to these papers, magmatic Li–Fe micas from the Krušné Hory well conforms values published by Bea et al. (1994).

REE budget in granites

In order to obtain a fairly objective opinion about the contributions of individual minerals to the total REE content in the rock, we combined the TIMA values of the modal content of minerals with EPMA and LA-ICP-MS analyses of REE in all minerals. The results for La, Ce, and Dy are shown in Supplementary Table S13 as contributions of individual minerals to the bulk rock content in ppm by weight.

To calculate the contributions of rock-forming silicates and apatite, we exclusively used the data obtained in this study. In the case of other minerals, we also used previously

published data from identical rocks types (Breiter et al. 2009; Breiter 2016; Breiter & Förster 2021) to increase the statistical significance of the data. To estimate the contribution of "other REE minerals", i.e., REE-bearing mineral grains not perfectly identified by TIMA, we used the average data of bastnäsite, which is the closest of the analyzed minerals to the not-exactly determined phases. The contribution of quartz is considered to be negligible; the REE contents in quartz are mostly below the detection limit of LA-ICP-MS, (author's data). Scarcely published REE data from quartz (obtained using ICP-MS after dissolution) indicate the preferential bound of REE to fluid inclusions, not to the mineral lattice, and their sum is typically lower than 0.5 ppm (Götze et al. 2021).

Supplementary Table S13 shows that the calculated sums of contributions of all mineral are usually significantly underestimated. The two exceptions are samples 4603 and 4688, both of which have undergone hydrothermal alteration of the important primary REE carrier, fluorite. The reason for the overestimation of our calculations is most likely the inhomogeneous distribution of late REE minerals. Rock chemical analysis from a 5–10 kg heavy sample is truly representative, whereas the area of a standard thin section does not represent, due to uneven REE distribution, a sufficient volume of the rock. A closer look will show that the overestimation is caused mainly by the high sum of "other REE-phases" and fluorite. Since these "other phases" are formed at the expense of the release of REE from primary fluorite according to the scheme REE-rich fluorite→REE-free fluorite+bastnasite+"other REE phases", the core of the problem is the proportion of the fresh primary vs. of the altered fluorite, which cannot be reliably quantified.

In order to generally verify the correctness of our REE-budget calculations, we made the same calculations for several other elements as well (Supplementary Table S14). Zirconium, effectively present only in the mineral zircon, is the simplest example: here, there is a match between the calculated and analyzed content, with the exception of sample #4743, which is very good. Phosphorus, however, represents the opposite extreme: its calculated contents in phosphates are in all cases much lower than the analyzed whole-rock system. The explanation of this discrepancy is simple: a large portion of phosphorus is hosted in alkali feldspar (London 1992) in values up to >1 wt.% P_2O_5. However, the binding of P in feldspar is unstable, and even with weak alteration, P is intensively, but unevenly released (Breiter et al. 2002). Therefore, any attempt to calculate the P-budget, including feldspar, would be doomed to failure. The best agreement between the calculated and analyzed contents we found was in the case of fluorine, which was effectively hosted particularly in micas and fluorite and subordinately in apatite. This proves that the modal content of at least these minerals was determined correctly.

The reason for the "too low" calculation may also be the inhomogeneity of mineral distribution, but also the binding of REE to submicroscopic mineral grains, which cannot be detected by TIMA. Despite the mentioned inaccuracies in the absolute estimates, we can conclude that monazite is the principal carrier of LREE in strongly peraluminous rocks hosting 30–80 % of total REE. Monazite is complemented with allanite in less-fractionated peraluminous granites, while with albite, in the strongly fractionated ones. In the A-type granites, the most important LREE hosts are monazite and fluorite, as well as fluorocarbonates as products of fluorite alteration. Among the rock-forming silicates, the dominant LREE carrier is plagioclase (oligoclase, albite) hosting in the S-type granites 5–15 % of LREE; but in the A-type granites, only <5 % LREE. Contributions of K-feldspar and micas are an order of smaller magnitude. The HREE are much more represented in the A-type than in the S-type granites (Supplementary Table S2, Fig. 2). In the A-type granites, the dominant HREE (represented here by Dy) carrier is fluorite (in altered samples products of its alteration), complemented with zircon and xenotime in different proportions. In the S-type granites, HREE are distributed between zircon, xenotime and monazite. Contribution of feldspars and mica to HREE distribution is negligible.

Another REE carrier in evolved granites could be topaz. Data about the trace elements in topaz are scarce (Northrup & Reeder 1994; Wasim et al. 2011; Breiter et al. 2013; Schaub et al. 2023). The only published REE topaz data are those by Wasim et al. (2011) done by neutron activation. Gemmy topaz from market, i.e., without any information about geology, contained 5–20 ppm La, 5–1000 ppm Ce etc. These data do not seem very reliable, but they indicate that topaz may play a certain role in the distribution of REE. Unfortunately, topaz grains in the studied samples were too small for laser ablation, and REE contents too low for EPMA.

The only published REE budgets of granitoids, at least partially comparable with our methodology, are budgets of 12 granitoids of different geochemical characteristic (peraluminous to peralkaline) by Bea (1996). In strongly to mildly peraluminous granites, which contain Fe-mica as only dark minerals, Bea (l.c.) obtained very similar data: 90–95 % of LREE was hosted in accessory phases (dominantly monazite, +allanite and apatite in Ca-enriched rocks), and 5–10 % of LREE in feldspars. In more mafic rocks, amphibole+pyroxene may host up to 30 % of LREE at the expense of monazite. The HREE in Bea´s samples are hosted namely in zircon+xenotime+apatite in strongly peraluminous rocks, as well as in zircon+allanite+amphibole+clinopyroxene in mildly peraluminous Ca-richer granitoids. The main differences between Bea´s and our samples is the greater importance of apatite, and a complete lack of fluorite in samples analyzed by Bea (1996). Nevertheless, both studies agree in the main features of the distribution of REEs, i.e., in the predominance of monazite (+allanite) for LREE, and zircon+xenotime for HREE, as well as in the limited importance of feldspars.

Conclusions

The main results achieved can be summarized as follows:

- the importance of rock-forming silicates for REE distribution is limited; relatively highest contribution was found in

plagioclase (up to approx. 15 % of LREE in S-type granites);
- in the S-type granites, monazite (LREE) and xenotime+zircon (HREE) dominate. In Ca-richer facies, allanite is also important (LREE);
- in the A-type granites, monazite+fluorite (incl. its alteration products) dominate as LREE hosts, while fluorite (incl. its alteration products) with small contributions of zircon and xenotime host the HREE.

Acknowledgements: This study was supported by RVO 67985831 in Geological Institute of the Czech Academy of Sciences. Igor Petrík and one anonymous reviewer are thanked for their positive and inspiring reviews.

References

Achterberg E., Ryan C., Jackson S. & Griffin W. 2001: Data reduction software for LA-ICP-MS. *Laser Ablation ICP-MS in the Earth Science* 29, 239–243.

Ackerman L. 2005: Magmatic vs. hydrothermal origin of fluorites from Vlastějovice, Bohemian Massif. *Journal of the Czech Geological Society* 50, 35–40.

Badanina E.V., Trumbull R.B., Dulski P., Wiedenbeck M., Veksler I.V. & Syritso L.F. 2006: The behavior of rare-earth and lithophile elements in rare-metal granites: a study of fluorite, melt inclusions and host rocks from the Khangilay complex, Transbaikalia, Russia. *Canadian Mineralogist* 44, 667–692. https://doi.org/10.2113/gscanmin.44.3.667

Bea F. 1996: Residence of REE, Y, Th and U in granites and crustal protoliths; implications for the chemistry of crustal melts. *Journal of Petrology* 7, 521–552. https://doi.org/10.1093/petrology/37.3.521

Bea F., Pereira M.D. & Stroh A. 1994: Mineral leucosome trace-element partitioning in a peraluminous migmatite (a laser ablation-ICP-MS study). *Chemical Geology* 117, 291–312. https://doi.org/10.1016/0009-2541(94)90133-3

Bi X., Cornell D.H. & Hu R. 2002: REE composition of primary and altered feldspar from the mineralized alteration zone of alkaline intrusive rocks, western Yunnan Province, China. *Ore Geology Reviews* 19, 69–78. https://doi.org/10.1016/S0169-1368(01)00034-8

Breiter K. 1997: Teplice rhyolite (Krušné hory Mts., Czech Republic) Chemical evidence of a multiply exhausted stratified magma chamber. *Věstník Českého geologického Ústavu* 72, 205–213.

Breiter K. 2008: Mineral and textural evolution of subvolcanic A-type granite: Hora Svaté Kateřiny stock, Krušné Hory Mts., Czech Republic. *Zeitschrift für geologische Wissenschaften* 36, 365–382.

Breiter K. 2012: Nearly contemporaneous evolution of the A- and S-type fractionated granites in the Krušné hory/Erzgebirge Mts., Central Europe. *Lithos* 151, 105–121. https://doi.org/10.1016/j.lithos.2011.09.022

Breiter K. 2016: Monazite and zircon as major carriers of Th, U, and Y in peraluminous granites: Examples from the Bohemian Massif. *Mineralogy and Petrology* 110, 767–785. https://doi.org/10.1007/s00710-016-0448-0

Breiter K. & Förster H.J. 2021: Compositional variability of monazite–cheralite–huttonite solid solutions, xenotime, and uraninite in geochemically distinct granites with special emphasis to the strongly fractionated peraluminous Li–F–P-rich Podlesí granite system (Erzgebirge/Krušné Hory Mts., Central Europe). *Minerals* 11, 127. https://doi.org/10.3390/min11020127

Breiter K., Sokolová M. & Sokol A. 1991: Geochemical specialization of the tin-bearing granitoid massifs of NW Bohemia. *Mineralium Deposita* 26, 298–306. https://doi.org/10.1007/BF00191077

Breiter K., Förster H. & Seltmann R. 1999: Variscan silicic magmatism and related tin-tungsten mineralization in the Erzgebirge–Slavkovský les metallogenic province. *Mineralium Deposita* 34, 505–521. https://doi.org/10.1007/s001260050217

Breiter K., Frýda J. & Leichmann J. 2002: Phosphorus and rubidium in alkali feldspars: case studies and possible genetic interpretation. *Bulletin of the Czech Geological Survey* 77, 93–104.

Breiter K., Müller A., Leichmann J. & Gabašová A. 2005: Textural and chemical evolution of a fractionated granitic system: the Podlesí stock, Czech Republic. *Lithos* 80, 323–345. https://doi.org/10.1016/j.lithos.2003.11.004

Breiter K., Čopjaková R. & Škoda R. 2009: The involvement of F, CO_2-, and As in the alteration of Zr–Th–REE-bearing accessory minerals in the Hora Svaté Kateřiny A-type granite, Czech Republic. *Canadian Mineralogist* 47, 1375–1398. https://doi.org/10.3749/canmin.47.6.1375

Breiter K., Gardenová N., Vaculovič T. & Kanický V. 2013: Topaz as an important host for Ge in granites and greisens. *Mineralogical Magazine* 77, 403–417.

Breiter K., Korbelová Z., Chládek Š., Uher P., Knesl I., Rambousek P., Honig S. & Šešulka V. 2017: Diversity of Ti–Sn–W–Nb–Ta oxide minerals in the classic granite-related magmatic–hydrothermal Cínovec/Zinnwald Sn–W–Li deposit (Czech Republic). *European Journal of Mineralogy* 29, 727–738. https://doi.org/10.1127/ejm/2017/0029-2650

Broska I. & Kubiš M. 2018: Accessory minerals and evolution of tin-bearing S-type granites in the western segment of the Gemeric Unit (Western Carpathians). *Geologica Carpathica* 69, 48–497. https://doi.org/10.1515/geoca-2018-0028

Broska I. & Uher P. 1991: Regional typology of zircon and their relationship to allanite-monazite antagonism (on example of Hercynian granitoids of the Western Carpathians). *Geologica Carpathica* 42, 271–277.

Broska I., Petrík I. & Williams C.T. 2000: Coexisting monazite and allanite in peraluminous granitoids of the Tríbeč Mountains, Western Carpathians. *American Mineralogist* 85, 22–32. https://doi.org/10.2138/am-2000-0104

Broska I., Williams C.T., Janák M. & Nagy G. 2005: Alteration and breakdown of xenotime-(Y) and monazite-(Ce) in granitic rocks of the Western Carpathians, Slovakia. *Lithos* 82, 71–83. https://doi.org/10.1016/j.lithos.2004.12.007

Cherniak D.J. 2003: REE diffusion in feldspar. *Chemical Geology* 193, 25–41. https://doi.org/10.1016/S0009-2541(02)00246-2

Förster H.-J. 1998a: The chemical composition of REE–Y–Th-U-rich accessory minerals in peraluminous granites of the Erzgebirge–Fichtelgebirge region, Germany, Part I: The monazite-(Ce)–brabantite solid solution series. *American Mineralogist* 83, 259–272. https://doi.org/10.2138/am-1998-3-409

Förster H.-J. 1998b: The chemical composition of REE–Y–Th–U-rich accessory minerals in peraluminous granites of the Erzgebirge–Fichtelgebirge region, Germany, Part II: Xenotime. *American Mineralogist* 83, 1302–1315. https://doi.org/10.2138/am-1998-11-1219

Förster H.-J. 2006: Composition and origin of intermediate solid solutions in the system thorite–xenotime–zircon–coffinite. *Lithos* 88, 35–55.

Förster H.-J. & Rhede D. 2006: The Be–Ta-rich granite of Seiffen (eastern Erzgebirge, Germany): Accessory-mineral chemistry, composition and age of a late-Variscan Li–F granite of A-type affinity. *Neues Jahrbuch für Mineralogy, Abhandlungen* 182, 307–321. https://doi.org/10.1127/0077-7757/2006/0055

Förster H.-J., Tischendorf G., Trumbull R.B. & Gottesmann B. 1999: Late-collisional granites in the Variscan Erzgebirge, Germany. *Journal of Petrology* 40, 1613–1645. https://doi.org/10.1093/petroj/40.11.1613

Förster H.-J., Gottesmann B., Tischendorf G., Siebel W., Rhede D., Seltmann R. & Wasternack J. 2007: Permo-Carboniferous subvolcanic rhyolitic dikes in the western Erzgebirge/Vogtland, Germany: a record of source heterogeneity of post-collisional felsic magmatism. *Neues Jahrbuch für Mineralogie, Abhandlungen* 183, 123–147. https://doi.org/10.1127/0077-7757/2007/0064

Förster H.-J., Rhede D. & Hecht L. 2008: Chemical composition of radioactive accessory minerals: Implications for the evolution, alteration, age, and uranium fertility of the Fichtelgebirge granites (NE Bavaria, Germany). *Neues Jahrbuch für Mineralogy, Abhandlungen* 185, 161–182. https://doi.org/10.1127/0077-7757/2008/0117

Götze J., Pan Y. & Müller A. 2021: Mineralogy and mineral chemistry of quartz: a review. *Mineralogical Magazine* 85, 639–664. https://doi.org/10.1180/mgm.2021.72

Heinrich W., Andrehs G. & Franz G. 1997: Monazite–xenotime miscibility gap thermometry: I. An empirical calibration. *Journal of Metamorphic Geology* 15, 3–17. https://doi.org/10.1111/j.1525-1314.1997.t01-1-00052.x

Hönig S., Čopjaková R., Škoda R., Novák M., Dolejš D., Leichmann J. & Galiová M.V. 2014: Garnet as a major carrier of the Y and REE in the granitic rocks: An example from the layered anorogenic granite in the Brno Batholith, Czech Republic. *American Mineralogist* 99, 1922–1941. https://doi.org/10.2138/am-2014-4728

Hoshino M, Watanabe Y. & Ishihara S. 2012: Crystal chemistry of monazite from the granitic rocks of Japan: Petrogenetic implications. *Canadian Mineralogist* 50, 1331–1346. https://doi.org/10.3749/canmin.50.5.1331

Hrstka T., Gottlieb P., Skála R., Breiter K. & Motl D. 2018: Automated mineralogy and petrology – applications of TESCAN Integrated Mineral Analyzer (TIMA). *Journal of Geosciences* 63, 47–63. https://doi.org/10.3190/jgeosci.250

Jarchovský T. 2006: The nature and genesis of greisen stocks at Krásno, Slavkovský les area – Western Bohemia, Czech Republic. *Journal of the Czech Geological Society* 51, 201–216.

Johan Z. & Johan V. 1994: Accessory minerals of the Cinovec (Zinnwald) granite cupola, Czech Republic: Part 1. Nb-, Ta- and Ti-bearing oxides. *Mineralogy and Petrology* 51, 323–343. https://doi.org/10.1007/BF01159735

Johan Z. & Johan V. 2005: Accessory minerals of the Cínovec (Zinnwald) granite cupola, Czech Republic: indicators of petrogenetic evolution. *Mineralogy and Petrology* 83, 113–150. https://doi.org/10.1007/s00710-004-0058-0

Kováříková P., Siebel W., Jelínek E., Holub F.V. & Blecha V. 2007: Petrology, geochemistry and zircon age for redwitzite at Abertamy, NW Bohemian Massif (Czech Republic): tracing the mantle component in Late Variscan intrusions. *Chemie der Erde* 67, 151–174. https://doi.org/10.1016/j.chemer.2007.04.002

Larsen R.B. 2002: The distribution of rare-earth elements in K-feldspar as an indicator of petrogenetic processes in granitic pegmatites: examples from two pegmatite fields in Southern Norway. *The Canadian Mineralogist* 40, 137–151. https://doi.org/10.2113/gscanmin.40.1.137

Li X., Zhang C., Wang L., Behrens H. & Holtz F. 2020: Experiments on the saturation of fluorite in magmatic systems. Implications for maximum F concentration and fluorine-cation bonding in silicate melt. *Journal of Earth Science* 31, 456–467. https://doi.org/10.1007/s12583-020-1305-y

Lipin B.R. & McKay G.A. (eds) 1989: Geochemistry and mineralogy of rare earth elements. *Reviews in Mineralogy* 21, 1–358. ISBN13 978-0-939950-25-6.

Linnemann U. & Romer R.L. 2010: Pre-Mesozoic geology of Saxo-Thuringia – from the Cadomian active margin to the Variscan orogen. *Schweizerbart*, Stuttgart.

Linthout K. 2007: Tripartite division of the system $2REEPO_4$–$CaTh(PO_4)_2$–$2ThSiO_4$, discredition of brabantite, and recognition of cheralite as the name for members dominated by $CaTh(PO_4)_2$. *Canadian Mineralogist* 45, 503–508. https://doi.org/10.2113/gscanmin.45.3.503

London D. 1992: Phosphorus in S-type magmas: The P_2O_5 content of feldspars from peraluminous granites, pegmatites and rhyolites. *American Mineralogist* 77, 126–145.

Makin S.A., Simandl G.J. & Marshall D. 2014: Fluorite and its potential as an indicator mineral for carbonatite-related rare earth element deposits. *British Columbia Geological Survey Paper* 2014-1, 207–212.

Mogilevsky P. 2007: On the miscibility gap in monazite–xenotime systems. *Chemical Geology* 34, 201–214. https://doi.org/10.1007/s00269-006-0139-1

Möller P., Parekh P.P. & Schneider H-J. 1976: The application of Tb/Ca–Tb/La abundance ratios to problems of fluorspar genesis. *Mineralim Deposita* 11, 111–116. https://doi.org/10.1007/BF00203098

Northrup P.A. & Reeder R.J. 1994: Evidence for the importance of growth-surface structure to trace element incorporation of topaz. *American Mineralogist* 79, 1167–1175.

Ondrejka M., Uher P., Pršek J. & Ozdín D. 2007: Arsenian monazite-(Ce) and xenotime-(Y), REE arsenates and carbonates from the Tisovec–Rejkovo rhyolite, Western Carpathians, Slovakia: Composition and substitutions in the $(REE,Y)XO_4$ system (X = P, As, Si, Nb, S). *Lithos* 95, 116–129. https://doi.org/10.1016/j.lithos.2006.07.019

Ren M., Parker D.F. & White J.C. 2003: Partitioning of Sr, Ba, Rb, Y, and LREE between plagioclase and peraluminous silicic magma. *American Mineralogist* 88, 1091–1103. https://doi.org/10.2138/am-2003-0718

René M. 2018: REE and Y mineralogy of the Krudum granite body (Saxothuringian zone). *Minerals* 8, 287. https://doi.org/10.3390/min8070287

Ritchie N.W. 2009: Spectrum Simulation in DTSA-II. *Microscopy and Microanalysis* 15, 454–468. https://doi.org/10.1017/S1431927609990407

Scaillet B. & Macdonald R. 2004: Fluorite stability in silicic magmas. *Contributions to Mineralogy and Petrology* 147, 319–329. https://doi.org/10.1007/s00410-004-0559-1

Schaub D.R., Northrup P., Nekvasil H., Catalano T. & Tappero R. 2023: Gas-mediated trace element incorporation into rhyolite-hosted topaz: A synchrotron microbeam XAS study. *American Mineralogist* 108, 2153–2163. https://doi.org/10.2138/am-2022-8417

Schönenberger J., Köhler J. & Markl G. 2008: REE systematisc of fluorides, calcite and siderite in peralkaline plutonic rocks from the Gardar Province, South Greenland. *Chemical Geology* 247, 16–35. https://doi.org/10.1016/j.chemgeo.2007.10.002

Schwinn G. & Markl G. 2005: REE systematics in hydrothermal fluorite. *Chemical Geology* 216, 225–248. https://doi.org/10.1016/j.chemgeo.2004.11.012

Seifert T. 2009: Metallogeny and petrogenesis of lamprophyres in the Mid-European Variscides: Post-collisional magmatism and its relationship to late-Variscan ore forming processes in the Erzgebirge (Bohemian Massif). *Millpress*, Amsterdam.

Seydoux-Guillaume A.M., Wirth R., Heinrich W. & Montel J.-M. 2002: Experimental determination of thorium partitioning between monazite and xenotime using analytical electron microscopy and X-ray diffraction Rietveld analysis. *European Journal of Mineralogy* 14, 869–878. https://doi.org/10.1127/0935-1221/2002/0014-0869

Štemprok M. 1986: Petrology and geochemistry of the Czechoslovak part of the Krušné Hory Mts. granite pluton. *Sborník Geologických Věd: Ložisková Geologie, Mineralogie* 27, 111–156.

Sun C. & Liang Y. 2017: A REE-in-plagioclase–clinopyroxene thermometer for crustal rocks. *Contributions to Mineralogy and Petrology* 172, 24. https://doi.org/10.1007/s00410-016-1326-9.

Taylor R.P. & Fallick A.E. 1997: The evolution of fluorine-rich felsic magma: source dichotomy, magmatic convergence and the origins of topaz granite. *Terra Nova* 9, 105–108. https://doi.org/10.1111/j.1365-3121.1997.00124.x

Tichomirowa M., Käßner A., Sperner B., Lapp M., Leonhardt D., Linnemann U., Münker C., Ovtcharova M., Pfänder J.A. & Schaltegger U. 2019: Dating multiply overprinted granites: The effect of protracted magmatism and fluid flow on dating systems (zircon U–Pb: SHRIMP/SIMS, LA-ICP-MS, CA-ID-TIMS; and Rb–Sr, Ar–Ar) – Granites from the Western Erzgebirge (Bohemian Massif, Germany). *Chemical Geology* 519, 11–38. https://doi.org/10.1016/j.chemgeo.2019.04.024

Tichomirowa M., Käßner A., Repstock A., Gerdes A. & Whitehouse M. 2022: New CA-ID-TIMS U–Pb zircon ages for the Altenberg–Teplice Volcanic Complex (ATVC) document discrete and coeval pulses of Variscan magmatic activity in the Eastern Erzgebirge (Eastern Variscan Belt). *International Journal of Earth Sciences* 111, 1885–1908. https://doi.org/10.1007/s00531-022-02204-2

Tischendorf G. 1989: Silicic Magmatism and Metallogenesis of the Erzgebirge. *Veröffentlichungen des Zentralinstituts für Physik der Erde* 107, 1–316.

Tomek F., Žák J., Svojtka M., Finger F. & Waitzinger M. 2019: Emplacement dynamics of syn-collapse ring dykes: An example from the Altenberg–Teplice caldera, Bohemian Massif. *Bulletin of GSA* 131, 997–116. https://doi.org/10.1130/B35019.1

Trinkler M., Monecke T., Thomas R. 2005: Constraints on the genesis of yellow fluorite in hydrothermal barite-fluorite veins of the Erzgebirge, Eastern Germany: evidence from optical absorption spectroscopy, rare-earth element data and fluid-inclusion investigations. *Canadian Mineralogist* 43, 883–898. https://doi.org/10.2113/gscanmin.43.3.883

Uher P., Plašienka D., Ondrejka M., Hraško L. & Konečný P. 2013: Uranium-rich monazite-(Ce) from the Krivá type granitic cobbles in conglomerates of the Pieniny Klippen Belt, Western Carpathians, Slovakia: Composition, age determination and possible source areas. *Geological Quarterly* 57, 343–352. https://doi.org/10.7306/gq.1089

Veksler I.V., Dorfman A.M., Kamenetsky M., Dulski P. & Dingwell D.B. 2005: Partitioning of lanthanides and Y between immiscible silicate and fluoride melts, fluorite and cryolite and the origin of the lanthanide tetrad effect in igneous rocks. *Geochimica et Cosmochimica Acta* 69, 2847–2860. https://doi.org/10.1016/j.gca.2004.08.007

Wasim M., Zafar W.A., Tufail M., Arif M., Daud M. & Ahmad A. 2011: Elemental analysis of topaz from northern Pakistan and assessment of induced radioactivity level after neutron irradiation for color induction. *Journal of Radioanalytical and Nuclear Chemistry* 287, 821–826. https://doi.org/10.1007/s10967-010-0879-8

Wasternack J., Märtens S. & Gottesmann B. 1995: Field and petrographic study of brecciation and greisenization phenomena in the Gottesberg tin deposit (Saxony, Germany). *Zeitschrift für Geologische Wissenschaften* 23, 619–642.

Weng Q., Niu H-C., Qu P., Shan Q., Li N-B. & Yang W-B. 2022: Mica compositional constraints on the petrogenesis and mineralization of the syenite-carbonatite complex in the Maoniuping REE deposit, SW China. *Ore Geology Reviews* 145, 104917. https://doi.org/10.1016/j.oregeorev.2022.104917

Electronic supplementary material is available online:
Supplementary Table S1 at http://geologicacarpathica.com/data/files/supplements/GC-75-2-Breiter_TableS1.docx
Supplementary Tables S2–S14 at http://geologicacarpathica.com/data/files/supplements/GC-75-2-Breiter_TablesS2-S14.docx